A NOVEL APPROACH OF TORNADO DETECTION USING A MACHINE INTELLIGENCE SYSTEM BASED ON SHEAR AND SPECTRAL SIGNATURES

Yadong Wang[1,*], Tian-You Yu[1], Mark Yeary[1], Alan Shapiro[2], Shamim Nemati[3], Michael Foster[4], David L. Andra Jr.[4], Michael Jain[5]

[1] School of Electrical and Computer Engineering, University of Oklahoma, Norman, Oklahoma, USA
[2] School of Meteorology, University of Oklahoma, Norman, Oklahoma, USA
[3] Department of Mathematics, University of Oklahoma, Norman, Oklahoma, USA
[4] National Weather Service, Norman, Oklahoma, USA
[5] National Severe Storms Laboratory, Norman, Oklahoma, USA

1. INTRODUCTION

The subjective detection of potentially tornadic storms using hook shape returns in a radar's display was first documented by Stout and Huff [1953], and was suggested as an indicator of tornadoes after the Illinois tornado [Fujita, 1958]. However, Forbes [1981] found that more than half of the tornadoes in his study did not exhibit apparent hook signatures and suggested that hook echoes may not be a reliable indicator. A unique feature of a strong azimuthal velocity difference at a constant range, termed tornado vortex signature (TVS), was first observed by [Burgess et al., 1975; Brown et al., 1978] using a pulsed Doppler radar. It has been shown that the probability of detection (POD), and the warning lead time for tornadoes in the United States were improved after the installation of the national network of Weather Surveillance Radar-1988 Doppler (WSR-88D) radars [Polger et al., 1994; Bieringer and Ray, 1996; Simmons and Sutter, 2005]. The basic idea of the current tornado detection algorithm (TDA) is to search for strong and localized azimuthal shear in the field of mean radial velocities [e.g., Crum and Alberty, 1993; Mitchell et al., 1998]. However, because of the smoothing effect of the radar resolution volume, the shear signature is degraded if the size of tornado is small and/or the tornado is located at far ranges [Brown and Lemon, 1976]. Recently, Brown et al. [2002] demonstrated that shear signature can be enhanced using half-degree angular sampling despite the expense of increasing statistical errors in velocity data.

The pioneering work of Zrnić and Doviak [1975] has shown that tornado spectra can have distinct signatures that set them apart from other weather spectra. The wide and bimodal tornado spectral signature (TSS) were subsequently verified by a pulsed Doppler radar with a significant maximum unambiguous velocity of approximately 90 $\mathrm{m\,s^{-1}}$[Zrnić et al., 1977; Zrnić and Istok, 1980; Zrnić et al., 1985]. Recent studies have shown that wide and flattened spectra are observed in a tornadic region using simulations and data collected from the research WSR-88D (KOUN) operated by the National Severe Storms Laboratory (NSSL) [Yu et al., 2007]. In that study, three complementary feature parameters that were derived from high-order spectral analysis and signal statistics were introduced to quantify TSS. It was suggested that the TSS can still be significant enough to facilitate tornado detection at far ranges, even though the shear signature may become difficult to identify. Additionally, the eigen-ratio of the correlation matrix derived from the raw time series data also have a distinct distribution in the tornadic region due to the wide and flat features of the spectrum [Yeary et al., 2007].

Although the tornadic signatures described above have the potential to facilitate tornado detection, each of these signatures has different characteristics and it is desirable to integrate them to improve the detection. A fuzzy logic methodology is ideal to address a complicated system which launches a decision based on multiple inputs simultaneously. Fuzzy logic based systems have already been widely applied to weather radar for hydrometeor classification [e.g., Vivekanandan et al., 1999; Liu and Chandrasekar, 2000; Zrnić et al., 2001]. In this work, a fuzzy logic system is developed to integrate tornadic signatures in both the spectral and velocity domains. The system is further enhanced by a feedback process provided through a neural network and is termed the neuro-fuzzy tornado detection algorithm (NFTDA).

This paper is organized as follows. The overview of TSS and NFTDA technique is developed in section 2 and is followed by the simulation results in section 3. The performance of NFTDA is further demonstrated using time series data collected by the KOUN radar in section 4. Finally, a summary and conclusions are given in section 5.

* *Corresponding author address:* Yadong Wang, University of Oklahoma, School of Electrical and Computer Engineering, University of Oklahoma, Norman, Oklahoma 73019; e-mail: wyd@ou.edu

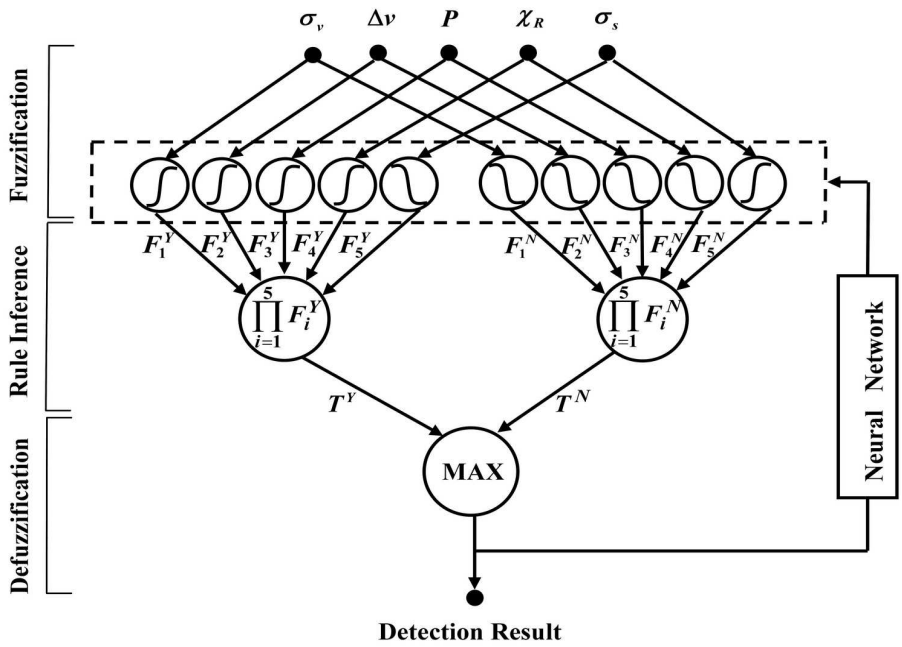

Figure 1: A schematic diagram of NFTDA. A fuzzy logic system is designed to detect a tornado, while a neural network is incorporated to refine the membership functions through a hybrid self-learning process.

2. NEURO-FUZZY TORNADO DETECTION ALGORITHM (NFTDA)

2.1. An Overview of Tornado Spectral Signatures

TSS with bimodal or white noise like features have been observed from both real data and analytical simulations [e.g., Zrnić and Doviak, 1975; Zrnić et al., 1985; Yu et al., 2007]. It is noted that the Doppler spectrum represents a distribution of weighted radial velocities within the radar resolution volume, and the mean Doppler velocity is defined by its statistical average (i.e., the first moment). It has been hypothesized [Yu et al., 2007] that the TSS can retain enough information to facilitate tornado detection, while the TVS is smoothed within the radar resolution volume and becomes difficult to identify. Three feature parameters were proposed by Yu et al. [2007] to characterize the TSS. The first parameter is spectrum width (σ_v), the second moment of a spectrum. Although the spectrum width is an intuitive parameter to describe the wide signature, it is not sufficient to characterize the shape of a tornadic spectrum and is susceptible to a number of factors such as inaccurate estimate of noise level and radar settings [Fang et al., 2004]. Moreover, large spectrum widths can be observed in a non-tornadic region where strong shear and/or low signal to noise ratio (SNR) are present. Two additional feature parameters, the phase of the radially integrated bispectrum (PRIB, denoted by P) and spectrum flatness σ_s, were introduced to characterize TSS [Yu et al., 2007]. Since most shape information of a pattern could be contained in the phase of its Fourier coefficients [Oppenheim and Lim, 1981] and the commonly used power spectrum (the second order spectrum) is phase blind. A third order spectrum termed "bispectrum" was introduced to extract the phase information by considering the Doppler spectrum in units of decibel (dB) as a sequence for pattern recognition [Yu et al., 2007]. The spectrum flatness, defined as the variance of a Doppler spectrum in dB, can be used to identify a white-noise like feature, which is often observed if the maximum unambiguous velocity is smaller than the maximum rotational speed of a tornado's vortex. In the cases considered [Yu et al., 2007], significantly high P and low σ_s values were obtained from spectra in a tornado compared to spectra from non-tornadic regions. Furthermore, Yeary et al. [2007] reported that a spectrum of white-noise like signature can reflect on the distribution of eigen-ratio of the correlation matrix estimated from the raw time series data. It is found that the regions of a large eigen-ratio (χ_R) are well correlated with wide and flat spectra in tornadic regions.

In this work, a fuzzy logic system is developed to integrate tornadic signatures, which includes the velocity

difference, spectrum width, spectral flatness, PRIB, and eigen-ratio.

2.2. Architecture of Neuro-Fuzzy Tornado Detection Algorithm

A fuzzy logic system can be considered as a non-linear mapping of feature parameters (i.e., inputs) to a binary output. In NFTDA the output is a binary detection of the presence of tornado. A typical fuzzy logic system can consist of three subsystems: fuzzification, rule inference, and defuzzification [Mendel, 1995]. A schematic diagram of the NFTDA is depicted in Fig. 1. In fuzzification, each feature parameter (or termed crisp input) is converted to a fuzzy variable with a value between $(0, 1)$, termed membership degree, by a membership function for each class. The fuzzy variables are the inputs to the subsystem of rule inference with an output of T^Y and T^N for tornadic and non-tornadic cases, respectively, as shown in Fig. 1. The relationship between the input and output of rule inference is described by fuzzy rules. The process of evaluating the strength of each rule is called *rule inference*. In the NFTDA, the Mamdani system is selected for the rule inference [Ross, 2005]. In this system the max-product (or correlation-product) is used to set the rule strength, which is defined as the product of the input fuzzy variables. Finally, the output of rule inference, which is still a fuzzy variable, is converted to a crisp output of precise quantity through the subsystem of defuzzification. A maximum defuzzifer, defined as the largest of T^Y and T^N, is implemented in NFTDA and the final, binary detection is made.

The membership function is one of the most important components in a fuzzy logic system. It can be obtained from intuition, inference, rank ordering, neural networks and inductive reasoning, for example [Ross, 2005]. In the NFTDA, the shape of the membership functions were determined using prior knowledge of the relationship between the feature parameters and fuzzy variables for both tornado and non-tornadoes. Therefore, only an S- or Z-shaped membership function is employed. Each membership function for a crisp input x is defined by two breaking points (x_1 and x_2). The curve with the positive slope is known as the "S" curve, while the curve with the negative slope is known as the "Z" curve. An S-shape membership of spectrum width for the tornadic case with the two breaking points is exemplified in the upper left panel of Fig. 2. The breaking points of each membership function are initialized based on the results of statistical analysis. Subsequently, the breaking points are adjusted through a training process using a neural network as depicted in Fig. 1 [Liu and Chandrasekar, 2000; Wang et al., 2005].

3. SIMULATION RESULTS

The NFTDA is tested and verified using the Level I time series data generated from a radar simulator developed by Yu et al. [2007]. A model Doppler spectrum is simulated based on the superposition of weighted scatterers' velocities in the radar resolution volume. The weights are determined by the reflectivity, antenna pattern, and range weighting function. If the radial velocity of a scatterer exceeds the maximum unambiguous velocity (v_a), it is aliased into the interval of $[-v_a\ v_a]$. Consequently, the time series data are obtained from the inverse Fourier transform of the model spectrum with desirable SNR. A detailed description of the simulation is provided in Yu et al. [2007]. In this work, a tornado located at 1 km southwest of a mesocyclone is simulated. Both a tornado and mesocyclone are modeled by a Rankine combined vortex model with a maximum tangential velocity of 50 m s^{-1}and 15 m s^{-1}, respectively. The radius of the mesocyclone is 2 km and three different tornado's radius (r_t) are used in the simulation. Moreover, uniform reflectivity is applied to the tornado and a broad Gaussian-shape reflectivity is used for the mesocyclone. The level I data is simulated for a WSR-88D radar with one degree beamwidth (θ_b) and 250 m range resolution (ΔR). A maximum unambiguous velocity of 35 m s^{-1}indicates the presence of velocity aliasing. The mean Doppler velocities and spectrum widths are estimated by the autocovariance method [Doviak and Zrnić, 1993]. The spectral flatness, PRIB, and eigen-ratio are estimated by the methods described in Yu et al. [2007] and Yeary et al. [2007].

It has been shown that tornado's shear and spectral signatures depend on several factors such as the range, the tornado size, and the location of a tornado in the radar's resolution volume [e.g., Zrnić et al., 1977; Brown et al., 2002; Yu et al., 2007]. In this work, the ratio of detection, defined as $ROD = N_d/N_t$, is introduced to quantify the performance of NFTDA, where N_t is the total number of tornadic cases generated for the test and N_d is the number of cases detected. For each realization 121 tornado locations in the radar resolution volume are simulated with 11×11 grids in azimuthal and range directions at a given range (i.e., $N_t = 121$). The radar resolution volume of interest is centered at azimuth of 0 °. In order to calculate the velocity difference, signals from two additional volumes centered at azimuth angles of -1 °and 1 °are simulated at each range. For each tornado location, the five feature pa-

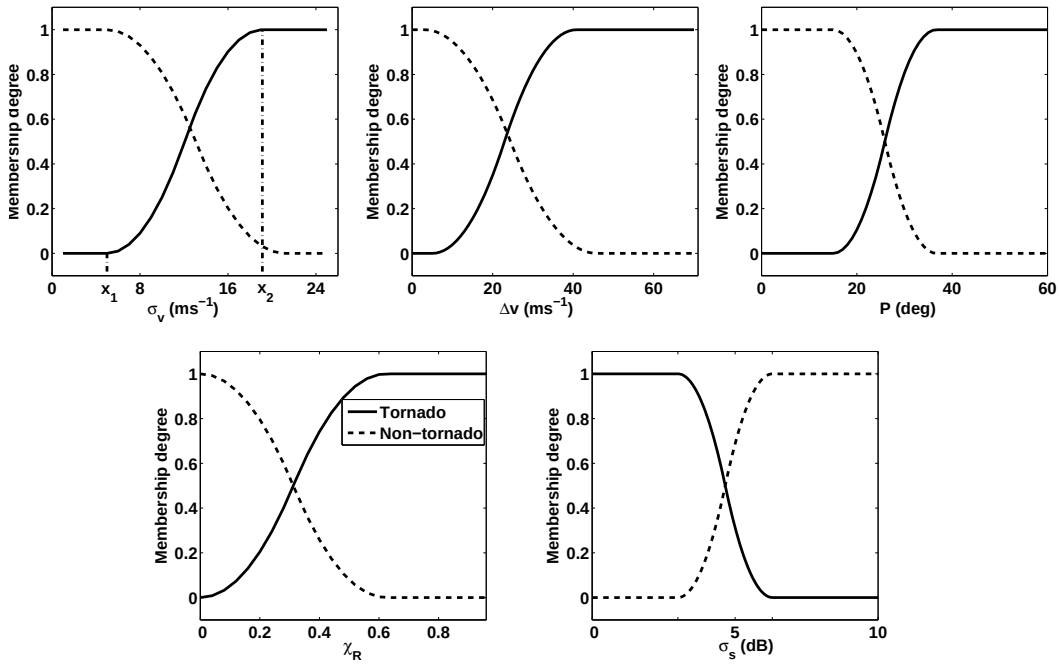

Figure 2: Membership functions for tornado and non-tornadic cases: spectrum width (upper left), velocity difference (upper middle), P (upper right), eigen-ratio (lower left), spectral flatness (lower right).

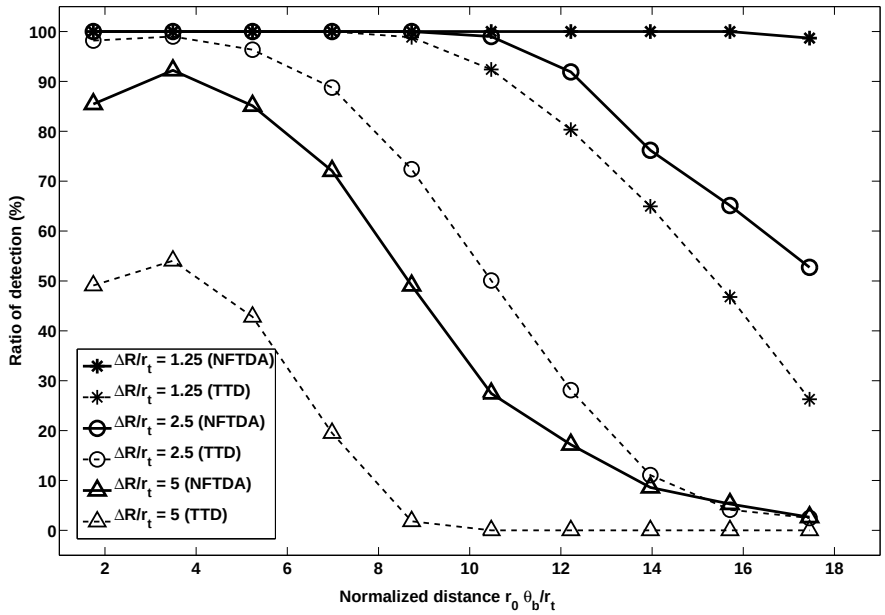

Figure 3: Statistical analysis of the performance of NFTDA as a function of normalized range for $\Delta R/r_t = 1.25$, 2.5, and 5.0. The NFTDA results are denoted by thick solid lines. The results from the detection based on a threshold of velocity difference of 20 m s^{-1}(TTD) are also provided for comparison and are denoted by the thin dashed lines.

rameters (velocity difference, spectrum width, spectral flatness, PRIB, and eigen-ratio) are obtained as the inputs of NFTDA. The ratio of detection represents the POD for different tornado's locations within the radar resolution volume. The ROD as a function of normalized range is presented in Fig. 3 for three tornado sizes that are defined by $\Delta R/r_t$, where r_t =50, 100, and 200 m. The normalized range is defined as $r_0\theta_b/r_t$, where r_0 is the range from the radar to the tornado and θ_b is in radian. Each data point represents the mean of ROD from 50 realizations, each one with different noise sequence in the time series data. Moreover, a tornado detection solely based on the thresholding of velocity difference is also implemented and is termed thresholding tornado detection (TTD). The ROD from the TTD using a threshold of 20 $\mathrm{m\,s^{-1}}$, one of the thresholds used in the NSSL TDA [Mitchell et al., 1998], is provided in Fig. 3 for comparison and is denoted by thin dashed lines. For $\Delta R/r_t = 1.25$ both NFTDA and TTD have superior RODs of approximately 100% when the normalized distance is smaller than 8.7. Beyond that, NFTDA can still have high RODs even though the shear signature is diminishing with increasing range. For the case of $\Delta R/r_t = 2.5$ NFTDA can still have a ROD of approximately 75% at a range of 80 km while the TTD has a ROD of 10%. It is evident that NFTDA provides higher RODs than TTD especially at far ranges for the three tornado sizes. It is because wide and flat spectra are still obtained from a tornadic vortex while the shear signature is degraded significantly. Although the performance of the TTD method can be improved by lowering the threshold, the false detections will be increased. In practice, several factors can limit the performance of NFTDA such as the degraded quality of the parameters at far ranges caused by the low SNRs, and the radar actually samples the storms aloft due to the earth curvature.

4. PERFORMANCE EVALUATIONS

4.1. Description Of The Experiments

The performance of the new NFTDA technique is further evaluated from two tornadic events in central Oklahoma that occurred on the 8 and 10 May 2003. The tornado outbreaks on 10 May are of primary interest because continuous time series data were collected by KOUN for the entire period. The National Climatic Data Center (NCDC) reported that three tornadoes from the same supercell thunderstorm broke out in central Oklahoma from 0329 UTC to 0425 UTC on 10 May 2003 (http://www4.ncdc.noaa.gov/cgi-win/wwcgi.dll?wwevent storms). The first tornado started at 0329 UTC and had traveled 18 miles during approximately 37 min before dissipating. The maximum Fujita scale of this tornado was reported at F3. The second tornado with a maximum of F1 scale began at approximately 4 miles south of Luther, Oklahoma at 0406 UTC and had lasted for approximately 9 minutes with 3 miles of track. The last tornado is the final segment of the previous tornado and had occurred between 0415 an 0424 UTC with a maximum scale of F0. The tornado damage path from the ground survey is displayed in Fig. 4 as the blue shaded area. In addition, the damage path of the May 8th tornado is denoted by the green shaded area. The NCDC has shown that this tornado with maximum magnitude of F4 which had traveled approximately 18 miles from 2210 UTC to 2238 UTC. However, the collection of time series data by KOUN started at approximately 2232 UTC and only two volume scans are associated with the tornado.

4.2. Experimental Results

All the feature parameters for NFTDA were calculated using raw time series data collected by KOUN in Norman, OK. The reflectivity, mean Doppler velocity, and spectrum width are calculated using the autocovariance method [Doviak and Zrnić, 1993]. The spectral features and the eigen-ratio are estimated by the methods described in Yu et al. [2007] and Yeary et al. [2007], respectively. NFTDA was subsequently applied to data from the lowest elevation angle of 0.5 °and with SNR is larger than 20 dB. The output of NFTDA is a binary detection of whether the tornado is present or not. The NSSL's TDA is also applied to the KOUN level II data for the comparisons and the results are defined by TDA-KOUN. Furthermore, detection results from the operational TDA of data from WSR-88D located at Twin Lakes, Oklahoma (KTLX) are included for comparisons and are defined as TDA-KTLX. The locations of KOUN and KTLX are also depicted in Fig. 4, where the KOUN located at origin point marked with a solid red star and the KTLX is marked with a solid black star. It is noted that the May 10th tornadoes were located closer to KTLX at all times. The time duration of one volume scan for KOUN and KTLX is 6 and 5 min, respectively. The time stamp shown in Fig. 4 for the two radars of KOUN and KTLX is color coded by red and black, respectively. The comparisons of NFTDA-KOUN and TDA-KOUN are divided into three time periods. In the first period, from 0329 UTC to 0353 UTC, the tornado was detected by both NSSL's TDA and NFTDA and the location of both detections agrees well with the tornado damage path. One exception is the TDA-KOUN at 0335 UTC, in which the location of the detection is approximately 1.25 km

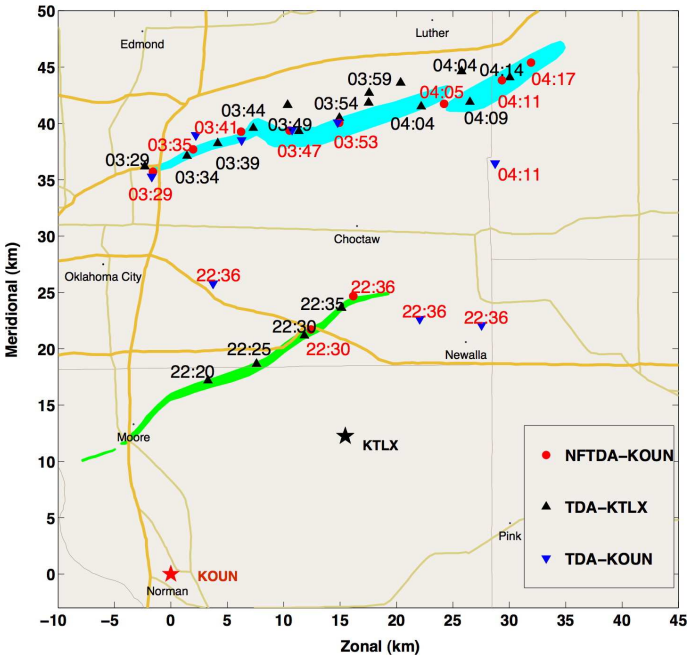

Figure 4: Comparisons of the detection results from TDA and NFTDA with KOUN data, which are denoted by blue triangles (TDA-KOUN) and red circles (NFTDA-KOUN), respectively for both tornadoes on May 8th and 10th, 2003. The tornado damage paths are depicted by green and light-blue shaded areas for the May 8th and May 10th cases, respectively. Moreover, the TDA results from the operational WSR-88D (KTLX) at Twin Lakes, OK are also shown.

from the edge of the damage path. The maximum detection range during this period is approximately 42.6 km. In the second period, from 0405 UTC to the demise of the third tornado at 0417 UTC, the TDA-KOUN has only one detection approximately 6 km away from the damage path at 0411 UTC. On the other hand, NFTDA-KOUN still provides robust and accurate detections that are consistent with the tornado damage path throughout the entire period. The maximum detection range of NFTDA in this period is 55.375 km. According to the NCDC, tornadoes were reported at F0-F1 scales during this period. The third period is for the volume scan at 0359 UTC and neither algorithms detected any tornado at this time. However, NFTDA identified a tornado at 19.4 km in zonal direction and 40.9 km in meridional direction, that is located within the damage path, from the data at the next elevation angle of 1.45 °. One hypothesis is that the tornado was at the dissipating stage and no longer researched the ground. These tornadoes showed uncontinuous tracks and lasted approximately 56 minutes, which is similar to the multiple cores mesocyclone described by Adlerman et al. [1999]. Furthermore, it is shown in Fig. 4 that the TDA from KTLX provides positive detections throughout the entire period. It is evident at least one positive detection agrees with the tornado damage path at any given time, although some false detections can be observed. The maximum range of detection for TDA-KTLX in this case is 32.1 km, which is consistent with the maximum detection of TDA-KOUN.

For the 8 May case, it is evident that NFTDA provides accurate detections for both times, while TDA-KOUN provides detections at 2236 UTC that are not consistent with damage path. In summary, it is clear that the TDA algorithm of both research and operational versions has suitable performance if a tornado is located at close range. The TDA-KOUN has limited performance when the tornado is weak or is located at distant ranges. On the other hand, the NFTDA is robust and can extend the tornado detection of NSSL TDA up to approximately 55 km.

5. SUMMARY AND CONCLUSIONS

It has been shown that strong azimuthal shears can be observed in a tornadic region and are the primary feature for the operational tornado detection algorithm of the WSR-88D. However, the shear signature deteriorates with range because of the smoothing effect by the increasing radar resolution volume. Recently, tornado spectral signatures (TSS) were characterized us-

ing spectrum width, bispectrum analysis, and signal statistics. Moreover, large eigen-ratios of the raw data in a range gate were also found to be associated with signals from the vicinity of a tornado. In this work a novel algorithm based on fuzzy logic is developed to integrate spectral, velocity, and eigen-ratio signatures with the goal of improving tornado detection. A fuzzy logic system is able to launch a decision based on simultaneous multiple inputs with fuzzy descriptions. The system is further enhanced by a training process of a neural network. This hybrid approach is termed Neuro-Fuzzy Tornado Detection Algorithm (NFTDA).

In the paper, the architecture of NFTDA was first presented and discussed. The feasibility of NFTDA was tested using numerical simulations for various conditions. The results indicated that the inclusion of tornado signatures, rather than shear information alone, is effective in improving tornado detection. Moreover, the performance of NFTDA was compared with the NSSL's TDA for the data collected by the KOUN radar during two tornadic events on the 8 and 10 May 2003. Tornado detection from the KTLX radar is also provided as a reference because it is located closer to the tornadoes than KOUN. Although only a limited number of cases was obtained, NFTDA has shown promising results in providing accurate detections that are consistent with the tornado damage path and TDA detections from KTLX with closer range and extending the detection range of NSSL's TDA. Furthermore, NFTDA is flexible to include additional feature parameters such as differential reflectivity and correlation coefficient from a dual-polarization radar. NFTDA can also be easily adopted by other radars of different characteristics such as beamwidth and range resolution without major modifications.

ACKNOWLEDGEMENT

This work was primarily supported by the DOC-NOAA NWS CSTAR program through the grant of NA17RJ1227. In addition, this work was supported in part by the National Science Foundation through ATM-0532107 and the Engineering Research Centers Program of the National Science Foundation under NSF Cooperative Agreement No. EEC-0313747. Any Opinions, findings and conclusions or recommendations expressed in this material are those of the author(s) and do not necessarily reflect those of the National Science Foundation. The authors would also like to thanks the NSSL staff for the collection of Level I data and the WFO in Norman for providing the ground damage survey.

References

Adlerman, E., Droegemeier, K., and Jones, R. (1999). A numerical simulation of cyclic mesocyclogenesis. *J. Atmos. Sci.*, 56:2045–2069.

Bieringer, P. and Ray, P. S. (1996). A comparison of tornado warning lead times with and without NEXRAD Doppler radar. *Wea. Forecasting*, 11:47–52.

Brown, R. A. (1998). Nomogram for aiding the interpretation of tornadic vortex signatures measured by Doppler radar. *Wea. Forecasting*, 13:505–512.

Brown, R. A. and Lemon, L. R. (1976). Single Doppler radar vortex recognition. part II: Tornadic vortex signatures. *17th Prepr. Radar Meteor. Conf.*, Seattle, WA. Amer. Meteor. Soc., 104-109

Brown, R. A., Lemon, L. R., and Burgess, D. W. (1978). Tornado detection by pulsed Doppler radar. *Mon. Wea. Rev.*, 106:29–38.

Brown, R. A., Wood, V. T., and Sirmans, D. (2002). Improved tornado detection using simulated and actual WSR-88D data with enhanced resolution. *J. Atmos. Oceanic Technol.*, 19:1759–1771.

Burgess, D. W., Lemon, L. R., and Brown, R. A. (1975). Tornado characteristics revealed by Doppler radar. *Geophys. Res. Lett.*, 183-184.

Burgess, D. W., Wood, V. T., and Brown, R. A. (1982). Mesocyclone evolution statistics. *12th Conf. on Severe Local Storms*, San Antonio, TX. Amer. Meteor. Soc., 422-424

Crum, T. D. and Alberty, R. L. (1993). The WSR-88D and the WSR-88D operational support facility. *Bull. Amer. Meteor. Soc.*, 74:1669–1687.

Doviak, R. J. and Zrnić, D. S. (1993). *Doppler Radar and Weather Observations*. Academic Press, San Diego, Calif., 562pp.

Fang, M., Doviak, R. J., and Melniko, V. (2004). Spectrum width measured by WSR-88D: Error sources and statistics of various weather phenomena. *J. Atmos. Oceanic Technol.*, 21:888–904.

Forbes, G. S. (1981). On the reliability of hook echoes as tornado indicators. *Mon. Wea. Rev.*, 109:1457–1466.

Fujita, T. (1958). Mesoanalysis of the Illinois tornadoes of 9 April 1953. *J. Atmos. Sci.*, 15:288–296.

Liu, H. and Chandrasekar, V. (2000). Classification of hydrometeors based on polarimetric radar measurements: Development of fuzzy logic and neuro-fuzzy system, and in-situ verification. *J. Atmos. Oceanic Technol.*, 17:140–164.

Marzban, C. and Stumpf, G. J. (1996). A neural network for tornado prediction based on Doppler radar-derived attributes. *J. Appl. Meteor.*, 35:617–626.

Mendel, J. M. (1995). Fuzzy logic systems for engineering: a tutorial. *Proc. IEEE*, 83:345–377.

Mitchell, E. D., Vasiloff, S. V., Stumpf, G. J., Witt, A., Eilts, M. D., Johnson, J. T., and Thomas, K. W. (1998). The National Severe Storms Laboratory tornado detection algorithm. *Wea. Forecasting*, 13:352–366.

Oppenheim, A. V. and Lim, J. S. (1981). The importance of phase in signals. *Proc. IEEE*, 69:529–541.

Polger, P. D., Goldsmith, B. S., and Bocchierri, R. C. (1994). National Weather Service warning performance based on the WSR-88D. *Bull. Amer. Meteor. Soc.*, 75:203–214.

Ross, T. J. (2005). *Fuzzy logic with engineering applications*. John Wiley & Sons, Ltd., 628pp.

Ryzhkov, A. V., Schuur, T. J., Burgess, D. W., and Zrnic, D. S. (2005). Polarimetric tornado detection. *J. Appl. Meteor.*, 44:557–570.

Simmons, K. M. and Sutter, D. (2005). WSR-88D radar, tornado warnings, and tornado casualties. *Wea. Forecasting*, 20:301–310.

Stout, G. E. and Huff, F. A. (1953). Radar records Illinois tornadogenesis. *Bull. Amer. Meteor. Soc.*, 34:281–284.

Vivekanandan, J., Zrnic, D. S., Ellis, S. M., Oye, R., Ryzhkov, A. V., and Straka, J. (1999). Cloud microphysics retrieval using s-band dual-polarization radar measurements. *Bull. Amer. Meteor. Soc.*, 80:381–388.

Wang, Y., Yu, T.-Y., Yeary, M., Shapiro, A., Zrnić, D., Foster, M., and D. L. Andra, J. (2005). Tornado detection using a neural-fuzzy method. *32nd Conf. on Radar Meteor.*, Albuquerque, NM. Amer. Meteor. Soc.

Yeary, M., Nemati, S., Yu, T.-Y., and Wang, Y. (2007). Tornadic time series detection using eigen analysis and a machine intelligence-based approach. *IEEE Trans. Geosci. Remote Sens.*, 4:335-339.

Yu, T.-Y., Wang, Y., Shapiro, A., Yeary, M., Zrnic, D. S., and Doviak, R. J. (2007). Characterization of tornado spectral signatures using higher order spectra. *J. Atmos. Oceanic Technol.*, accepted.

Zrnić, D. S., Burgess, D. W., and Hennington, L. D. (1985). Doppler spectra and estimated windspeed of a violent tornado. *J. Climate Appl. Meteor.*, 24:1068–1081.

Zrnić, D. S. and Doviak, R. J. (1975). Velocity spectra of vortices scanned with a pulsed-Doppler radar. *J. Appl. Meteor.*, 14:1531–1539.

Zrnić, D. S., Doviak, R. J., and Burgess, D. W. (1977). Probing tornadoes with a pulse Doppler radar. *Quart. J. Roy. Meteor. Soc.*, 103:707–720.

Zrnić, D. S. and Istok, M. (1980). Wind speeds in two tornadic storms and a tornado, deduced from Doppler spectra. *J. Appl. Meteor.*, 19:1405–1415.

Zrnić, D. S., Ryzhkov, A., Straka, J., Liu, Y., and Chandrasekar, V. (2001). Testing a procedure for automatic classification of hydrometeor types. *J. Atmos. Oceanic Technol.*, 18:892–913.